CHAPTER IV

EXPERIMENTAL RESULTS AND DISCUSSION I: ERBIUM-DOPED FIBER AMPLIFIER WITH OPTICAL COUNTER-FEEDBACK

4.1 INTRODUCTION

Wavelength division multiplexing (WDM) and erbium-doped fiber amplifiers (EDFAs) are key technologies to the new generation of high speed and large capacity optical fiber communication systems. The optical signal gain of a conventional EDFA depends on many parameters such as the input signal level, the pump power and signal wavelength. This causes signal power instability and crosstalk between different channels in multiwavelength optical networks where the number of channels and thus the total signal power vary as a result of channel adding and dropping [1-3]. The ability to automatically control the signals gain is thus important for the application of EDFAs in the optical networks. One effective approach for achieving this is to induce lasing at a particular wavelength in an EDFA system so that a constant average population inversion can be maintained [4-6]. As a result, the signals gain can be "clamped" within a wide range of input signal power. Such system is normally treated as a gain clamped amplifier [6-7], or a gain control amplifier [8-9]. Several techniques using ring configurations [5-7] and linear configurations [9] have been demonstrated.

In this chapter, erbium-doped fiber amplifier with the optical counter-feedback based on the ring configuration is presented. The original idea of this feedback direction was to eliminate the oscillating laser from the EDFA output [10]. However, we show that the laser cannot be completely eliminated due to the back reflection arising from passive components and splicing points in the cavity.

Next section describes the experimental setup for such a configuration. Section 4.3 starts from the demonstration of the amplifier performance without the wavelength selective element or tunable bandpass filter (TBF). Performance comparison among the systems: *system without TBF*, *system with TBF* and *system without optical feedback* is treated in Section 4.4. It was found that laser-induced saturation at the input end of erbium-doped fiber (EDF) played an important role in degradation of the noise figure in the unsaturated regime. The chapter ends with the study on the variation of the lasing wavelength for the system with TBF.

4.2 EXPERIMENTAL SETUP

The configuration for demonstrating the EDFA with optical feedback is shown in Fig. 4.1. The system consists of two 980/1550 nm wavelength division multiplexers (WDMs), three couplers: C_1 and C_2, with an output coupling ratio of 95%, and C_3 for monitoring the spectrum in an anti-clockwise direction from the 1% port. A unidirectional oscillation of the laser was achieved using an isolator, ISO 1. Fig. 4.1 shows a ***counter-feedback*** configuration where the laser oscillates in the direction opposite that of the input signal. Without the tunable band-pass filter (TBF), the system was treated as a *system without TBF* with the existence of both laser and amplified spontaneous emission (ASE) feedbacks, dominated by the oscillating mode

at the wavelength of 1558 nm. For the system with only a laser feedback (*system with TBF*), the TBF was placed in the cavity to block the ASE and allow only the selected mode (1558 nm in this case) to pass through, in order for comparison with the former system. For the *system without optical feedback*, the ring was opened at the arm between ISO 1 and C_3. A-15-m long EDF with a cutoff wavelength of 950 nm, a refractive index of 1.473 and an Er^{3+} concentration of +440 ppm was used as an active medium. Pump power was provided by a laser diode via the 980 nm port of WDM I. The system was characterized at the signal wavelength of 1550 nm. The signal source was from an ANDO AQ4321D tunable laser source (TLS). The amplified output signal was monitored using an ANDO AQ6317B optical spectrum analyzer (OSA). Time-Domain Extinction (TDE) Method was applied in the system characterization.

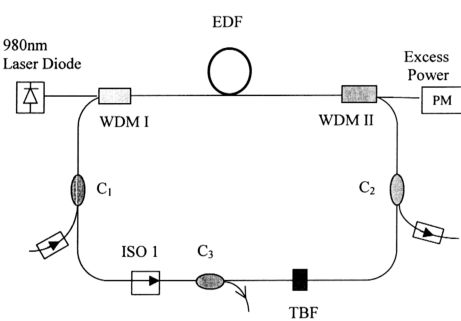

Fig. 4.1 *Experimental setup for demonstrating the EDFA system with optical counter-feedback. (EDF: erbium-doped fiber; WDM: wavelength division multiplexer; C: coupler; ISO: isolator; TBF: tunable bandpass filter; PM: power meter).*

The data presented in this chapter is referred to as *system value* where input and output coupling losses are included. The *intrinsic values* can be determined using the input and output coupling losses given in Chapter 3. Time-Domain-Extinction (TDE) method was used in the system characterization.

4.3 AMPLIFIER PERFORMANCE WITHOUT WAVELENGTH SELECTIVE ELEMENT

4.3.1 Output Spectrums

In the counter-feedback EDFA system, the oscillating laser is supposed to be eliminated at the EDFA output. However, the back reflection arising from the component terminations and splicing points, as mentioned in Section 3.3, causes the back reflected laser appearing at the EDFA output as shown in Fig. 4.2. There are two back reflected laser peaks at the wavelength of around 1558 nm at the pump power P_p = 134.5 mW. The mode at the wavelength of 1550 nm is the input signal with the power of P_{in} = –31.2 dBm.

Fig. 4.3(a) shows the oscillating laser monitored from the 1 % port of coupler C_3 in the anti-clockwise direction at P_p = 134.5 mW. There are two laser modes oscillating simultaneously. However, with a lower pump power, 50 mW for example, there is only one oscillation mode in the cavity as shown in Fig. 4.3(b). This can be explained from the gain competition [11]. Once a mode reaches the threshold, the gain of the mode is clamped at the value of loss. Since the gain is wavelength dependent and also not entirely homogeneous (spatially and spectrally) it is possible for other modes to reach the threshold and start oscillating at a higher pump. The oscillator can thus oscillate simultaneously in more than one mode, with each mode oscillating almost independent of the other.

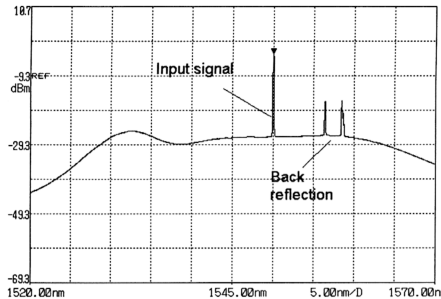

Fig. 4.2 *Output spectrum. The back reflection arising from the component terminations and splicing points causes the back reflected laser appearing at the EDFA output.*

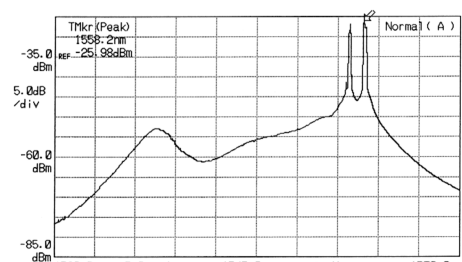

(a) *(continue...)*

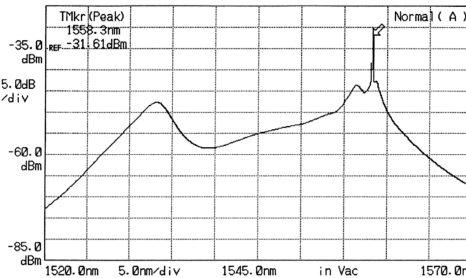

(b)

Fig. 4.3 *The oscillating laser monitored from the 1 % port of coupler C_3 in the anti-clockwise direction at the pump power of (a). 134.5 mW and (b). 50 mW.*

4.3.2 Effects of Pump Power Variation

The signal gain as a function of pump power at the input signal power P_{in} = –31.2 dBm and signal wavelength λ_{sig} = 1550 nm is illustrated in Fig. 4.4. At the low pump powers, the signal gain increases nearly linearly with the pump power. For $P_p >$ 27.1 mW, the signal gain is independent of the pump power. Within this pumping range, there is an oscillating laser in the anti-clockwise direction and the point when the signal gain becomes constant is corresponding to the condition of the onset of laser oscillation. Above this pump power, the metastable level population clamps at the threshold value. All of the additional pumping power then goes into the oscillating mode. Consequently, the input signal does not experience further amplification after the onset of laser oscillation.

As shown in Fig. 4.5, the noise figure increases by increasing the pump power. This can be attributed to the depletion of the population at the EDF input end caused by the increasing backward ASE with respect to the pump power. The noise figure increases from 6 dB at P_p = 13.4 mW to 7.7 dB at the maximum pump power P_p = 134.5 mW. Note that although the population is supposed to be clamped at its inversion after the onset of laser oscillation, spectral hole burning, introduced by the strong oscillating laser, causes an incomplete clamping of the sub-levels [4]. Another plausible reason is that the strength of the oscillating laser continuously increases with the pump power. Laser-induced saturation thus takes place at the EDF input end since it is the strongest at the EDF input end in the anti-clockwise direction. Depopulation at this portion results in degradation in the noise figure performance.

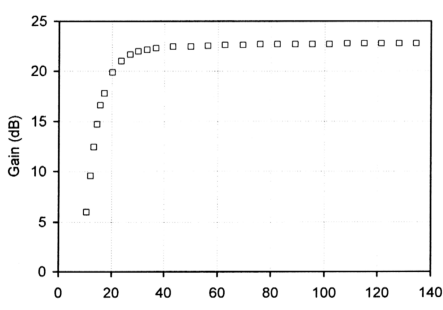

Fig. 4.4 *Signal gain as a function of pump power P_{in} = –31.2 dBm and λ_{sig} = 1550 nm.*

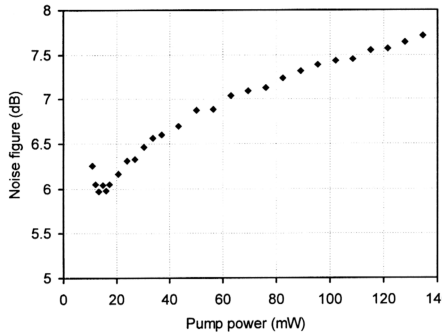

Fig. 4.5 *Noise figure as a function of pump power at P_{in} = –31.2 dBm and λ_{sig} = 1550 nm.*

4.3.3 Effects of Input Signal Power Variation

Signal gain as a function of input signal power for the pump powers P_p = 43.4 mW, 89 mW and 134.5 mW is illustrated in Fig. 4.6. In the unsaturated regime (small-signal regime), the signal gains are almost identical (~22.6 dB) for the different pump powers since these pump powers are above the lasing threshold. The largest dynamic range is achieved by the maximum pump power P_p = 134.5 mW. With this P_p, the strong oscillating laser in the cavity introduces a stronger gain-clamping effect to the input signal. As a result, input signal power as high as –4 dBm is required to cause the saturation of the amplifier system. The input saturation power P_{in}^{sat} is defined by 3 dB gain compression from the small-signal gain. The effect of gain saturation by the amplified signal occurs in a regime where the stimulated emission

rate induced by the high signal power becomes comparable to the pumping rate, or even takes over. This effect can be alleviated by increasing the pump power. For the smaller pump power P_p = 43.4 mW, an input signal power of only –10.5 dBm is enough to saturate the amplifier due to a weaker oscillating laser. For P_p = 89 mW, the input saturation power is determined to be P_{in}^{sat} = –6 dBm.

Fig. 4.7 shows the noise figure versus input signal power for different pump powers. The noise figure is higher for the higher P_p, consistent with the feature shown in Fig. 4.4. In the small signal regime, the noise figure for all the pump powers are fairly consistent. It is worth noting that when P_{in} approximates the saturated regime around P_{in}^{sat} = -5 dBm, there is a dip for each pump power. The dip effect arises from the suppression of the backward ASE by this input signal power [12-13]. The existing strong backward ASE at the small input signal powers at the high pump powers depletes the inversion at the EDF input end, causing a higher noise figure in the small-signal gain regime. Such effect is referred to as ASE *self-saturation* in Ref. [13] Suppression of the backward ASE by a higher input power restore the inversion to a higher level, thus improving the noise figure by 2.1 dB, 1.7 dB and 1.0 dB for the P_p = 134.5 mW, 89.0 mW and 43.4 mW respectively. The deepest dip is obtained when the effect of self-saturation is completely suppressed, which is in the case of P_p = 134.5 mW. The input signal power required to achieve the minimum noise figure is –8 dBm for P_p = 43.4 mW whereas for the higher P_p = 89 mW and 134.5 mW, a higher P_{in} = –4 dBm is required. The noise figures are expected to increase progressively if the higher P_{in} is applied as a result of signal-induced saturation [13].

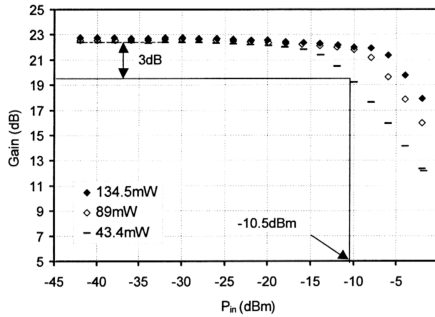

Fig. 4.6 *Signal gain as a function of input signal power for P_p = 43.4 mW, 89 mW and 134.5 mW.*

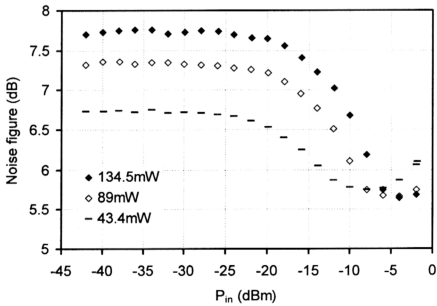

Fig. 4.7 *Noise figure as a function of input signal power for P_p = 43.4 mW, 89 mW and 134.5 mW.*

4.3.4 Effects of Signal Wavelength Variation

With a small input power of –31.2 dBm, the signal gain is studied as a function of signal wavelength as denoted in Fig. 4.8. Due to the gain clamping effect after the onset of the laser oscillation, the signal gains are almost identical for all the given pump powers P_p = 43.4 mW, 89 mW and 134.5 mW. The maximum signal gain of 23.4 dB is achieved at the signal wavelength of 1556 nm. With the small input signal power, the effect of saturation is negligible. Therefore, the gain spectral follows the ASE spectral profile as shown in Fig. 4.2.

In Fig. 4.9, the noise figure as a function of the signal wavelength is presented for different pump powers. The noise figures are high at the short signal wavelength. At the maximum pump power P_p = 134.5 mW, noise figure as high as 11.8 dB is obtained at λ_{sig} = 1520 nm. As referring to the ASE spectral profile in Fig. 4.2, the photons emission at this wavelength is small. This reveals a small population at the upper sublevels of metastable state, corresponding to the 1520 nm transition. The noise figures for all the different pump powers decrease with the signal wavelength due to the higher population at the bottom sublevels of metastable state according the Boltzmann distribution.

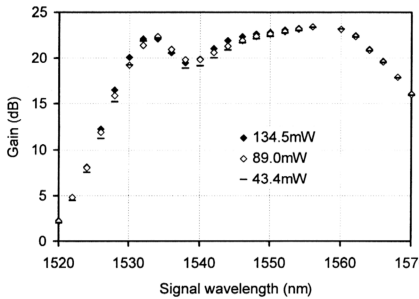

Fig. 4.8 *Signal gain as a function of signal wavelength with a small input power of $P_{in} = -31.2$ dBm.*

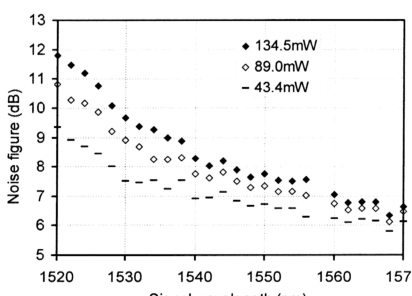

Fig. 4.9 *Noise figure as a function of signal wavelength with a small input power of $P_{in} = -31.2$ dBm.*

4.4 PERFORMANCE COMPARISON AMONG THE SYSTEMS

4.4.1 Output Spectrums

Previous section describes the EDFA system without the wavelength selective element (TBF). With the TBF in the ring cavity, the lasing wavelengths of the system can be selected. In this study, the oscillating laser is selected to be 1558 nm in order for comparing with the former configuration that without TBF which lase at the wavelength of 1558 nm. Both systems with the optical feedback were compared with the configuration without optical feedback, ie., with the ring open.

Fig. 4.10 depicts the output spectrum monitored from the EDFA output for the feedback configuration with TBF and without TBF and the system without feedback at the maximum available pump. The probe signal was injected at the wavelength of 1550 nm. Without the optical feedback, all of the photons re-emit as incoherent spontaneous emission. Some photons get amplified resulting in amplified spontaneous emission. By creating a feedback loop to the system, the power level for the ASE is clamped at the value it had at the oscillation threshold. From Fig. 4.10, it is evident that the ASE levels are much lower for the systems with the optical feedback as compared to the case without the optical feedback. The peaks at the wavelength around λ = 1558 nm are the back reflected lasers oscillating in the anti-clockwise direction. Fig. 4.11 shows the output spectrums in this direction monitored from the 1 % port of the coupler C_3 (see Fig. 4.1). Due to the mode competition effect, there are two laser peaks for the configuration without the TBF. The power level around these laser peaks is relatively high due to the amplification of the ASE through the circulation. With the TBF, the mode competition is enhanced and only a mode at the wavelength of 1558 nm is allowed to oscillate.

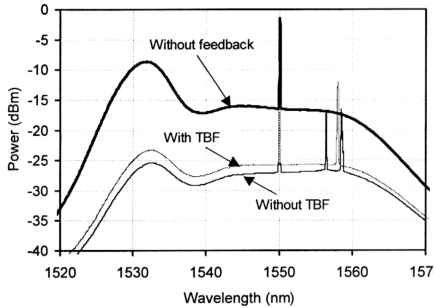

Fig. 4.10 *Output spectrum monitored from the EDFA output for the feedback configuration with TBF and without TBF and the system without feedback at the maximum pump power P_p= 134.5 mW.*

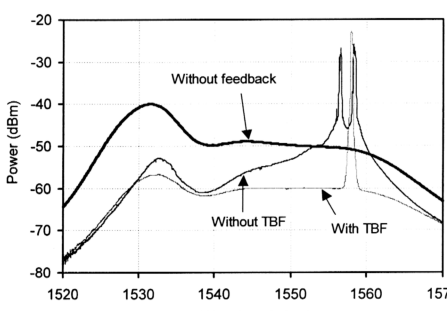

Fig. 4.11 *Output spectrums in the anti-clockwise direction monitored from the 1 % port of the coupler C_3.*

4.4.2 Effects of Pump Power Variation

The signal gain as a function of pump power is depicted in Fig. 4.12. The input signal power and signal wavelength is P_{in} = –31.2 dBm and λ_{sig} = 1550 nm, respectively. After the onset of laser oscillation, both systems with optical feedback exhibit the gain clamping effect where the signal gains are independent of the pump power. With the TBF, a higher loss is introduced to the system. Therefore, a higher gain is required to achieve the loss in order to fulfill the condition of laser oscillation. As shown in Fig. 4.12, the system with the TBF achieves the signal gain of 24.3 dB, 1.5 dB higher than that of the system without TBF. More pump power has been absorbed to provide this additional gain. This can be seen from Fig. 4.13 where the excess pump power is the lowest for the system with TBF. Without the optical feedback, laser oscillation is impossible for the available pump power. Under this condition, increasing the pump power will thus increase the population at the metastable level. This results in continuously increase in the signal gain. In this case, the signal gain as high as 34 dB is achieved at the maximum available pump power of 134.5 mW. The absorbed pump power in this system is also the lowest. With the optical feedbacks, the simulation results start to deviate from the experimental data after the oscillation threshold with the former achieves the gain ~2 dB higher than the latter.

Power conversion efficiency (PCE) as a function of the pump power is illustrated in Fig. 4.14. PCE is an important parameter indicating the saturation characteristics of the EDFs. A high PCE can be achieved when a conventional single-pass EDFA is operated under highly saturated regime [14]. Operating in such a regime, the EDFA is normally used as a power amplifier [12, 14] in order to yield a

maximized output signal power. The PCE is defined as [13]

$$PCE(\%) = \frac{P_{out} - P_{in}}{P_p} \tag{4.1}$$

where P_{out}: amplified output signal power, P_{in} : input signal power, P_p : pump power. The PCE as a function of pump power for different schemes is denoted in Fig. 4.14. The input signal used was P_{in} = –31.2 dBm. Without the optical feedback, the PCE increases to 1.45 % at $P_p \approx 62.9$ mW and starts to saturate until the maximum available pump of 134.5 mW. Initially, the PCEs for the systems with optical feedback increase linearly, similar to the case without feedback. It is worth noting that at the pump power $P_p > 23$ mW, the PCEs for the systems with optical feedback start to depart from that of the system without optical feedback. The maximum PCE of 0.4 % is achieved at P_p = 27 mW for the system without TBF. With the TBF, a higher maximum PCE of 0.7 % is achieved at P_p = 23.8 mW. From the laser theory, it is stated that the additional pumping power will be converted into the oscillating laser mode above the lasing threshold. Efficiency of the power conversion to the input signal thus reduces after the threshold. The pump powers P_p = 23.8 mW and 27 mW thus correspond to the threshold of the onset of laser oscillation for the systems with and without TBF, respectively. Although the threshold is supposed to be higher in the system with TBF as compared to the system without TBF, the pump needed is compensated by the higher pump absorption as shown in Fig. 4.13.

As demonstrated by R. G. Smart et. al. [12], the noise figure increased by increasing the pumping power for co-pumping scheme due to the depopulation at the EDF input end caused by the increasing backward ASE with respect to the pump power. The simulation results also exhibit the same property. Although the gain

increases with the pump power, an increase in gain results in an almost proportional increase in ASE, which then causes noise degradation as given in Eq. 2.64. The cross signs in Fig. 4.15 that represents the scheme without optical feedback shows this pump power dependent feature. Maximum noise figures of 7.7 dB, 7.2 dB and 6.6 dB have been achieved at the maximum available pump at P_{in} = –31.2 dBm, for the system without TBF, system with TBF and system without optical feedback, respectively. In the system without feedback, degradation of the noise figure is mainly due to the ASE self-saturation at the EDF input end. It has been reported that self-saturation by backward ASE can be partially suppressed by using a midway isolator somewhere between the EDF [12]. Existence of the midway isolator prevents the backward ASE generating from the EDF output end, thus reducing the self-saturation effect. However, such approach is not applicable in the system with optical counter-feedback. Besides the ASE self-saturation at the EDF input end, degradation of the noise figure in the feedback schemes with respect to the pump is mainly caused by the saturation induced by the strong oscillating laser mode at the EDF input end. Note that although the population is supposed to be clamped at its inversion level after the onset of the laser oscillation, spectral hole burning, introduced by the strong oscillating laser, causes an incomplete clamping of the sublevels [4]. Therefore, a slight variation of the population is expected due to the different level of the laser strength. The laser strength increases with the pump since all of the additional pumping power fed into this level after the lasing threshold goes into the oscillating laser mode. As a result, saturation effect increases and noise figure increases accordingly. The higher noise figure in the system without TBF could be due to the lower inversion since a lower signal gain is obtained as shown in Fig. 4.12.

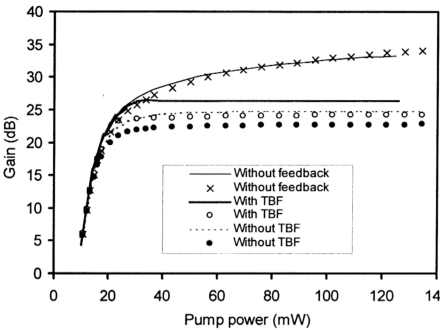

Fig. 4.12 *Signal gain as a function of pump power. The input signal power and signal wavelength is $P_{in} = -31.2$ dBm and $\lambda_{sig} = 1550$ nm, respectively. (Point signs: Measured results; lines: Simulation results).*

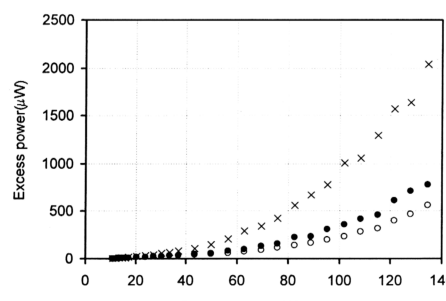

Fig. 4.13 *Excess pump power as a function of pump power. The input signal power and signal wavelength is $P_{in} = -31.2$ dBm and $\lambda_{sig} = 1550$ nm, respectively. (•: without TBF; o: with TBF; x: without feedback).*

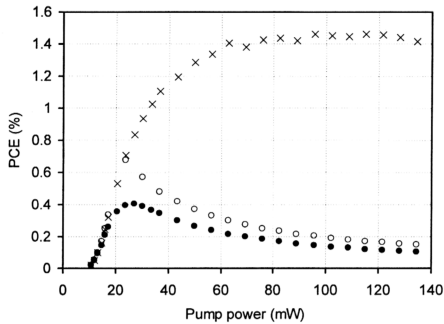

Fig. 4.14 *Power conversion efficiency as a function of the pump power. The input signal power and signal wavelength is P_{in} = –31.2 dBm and λ_{sig} = 1550 nm, respectively. (•: without TBF; o: with TBF; x: without feedback).*

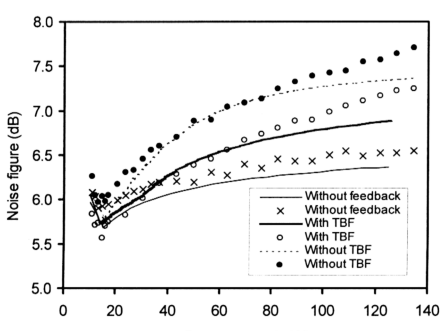

Fig. 4.15 *Noise figure versus pump power. The input signal power and signal wavelength is P_{in} = –31.2 dBm and λ_{sig} = 1550 nm, respectively. (Point signs: Measured results; lines: Simulation results).*

4.4.3 Effects of Input Signal Power Variation

Signal gain as a function of input signal power for different feedback schemes is denoted in Fig. 4.16. The systems were pumped at the maximum available power P_p = 134.5 mW. For the systems with optical feedback, small-signal gain is independent of the input signal power up to P_{in} = –6 dBm since the population at the metastable level is clamped at the threshold inversion. The gain compression of ~10 dB is observed in this unsaturated regime as compared to the system without feedback which achieves the maximum small-signal gain of 34.3 dB. Saturation input power markedly increases from P_{in}^{sat} = –19 dBm for the system without feedback, to P_{in}^{sat} = –5 dBm for the system with TBF and to P_{in}^{sat} = –4 dBm for the system without TBF. In this regime, the simulation results and the experimental data for all the schemes are identical. The significant increase in the dynamic range can be attributed to the strong clamping in the population, which fixes the signal gain up to a high input signal level of ~-6 dBm. Note that the multimode oscillation in the system without TBF enhances the gain clamping effect in which the saturation input powers increases by 1 dB as compared to the system with TBF. However, it is compensated at a cost of 1 dB in gain compression.

The noise figure characteristics from the unsaturated to the saturated input signal power are shown in Fig. 4.17. Similar to the conventional co-pumping scheme, the system without optical feedback shows a dip in the moderately saturated regime [12-13, 15], which is –5 dBm in our case. The dip effect arises from the suppression of the backward ASE by this saturating signal. This effect is also observed in the simulation results for all the schemes. The existing strong backward ASE at the small P_{in} results in self-saturation at the EDF input end, causing a higher noise figure in the

unsaturated regime. Suppression of the backward ASE by the saturating signal restores the inversion to a higher level thus improving the noise figure by ~1.1 dB in the system without feedback. The mechanism of such effect is that the saturating signal depletes the population of the EDF at the input region, resulting in significant decrease in the backward ASE. Therefore, the rate of saturation ordepopulation induced by this backward ASE is progressively reduced. As far as the rate of the backward ASE suppression by the saturating signal over come the rate of the ASE self-saturation, the inversion at the EDF input end can be restored back to a higher level. Generally, the decrease in the noise figure is observed only in the system with a high small-signal gain (i. e. > 30dB) [13]. However, with this counter-feedback scheme, the dips are distinct although the small-signal gains are only 22.8 dB and 24.5 dB for the system without TBF and the system with TBF, respectively. The corresponding depths of the dips in these cases are 2.1 dB and 2.0 dB, respectively. Note that in this regime gain clamping effect lost and the systems operated below the oscillation threshold as a result of gain quenching by the saturating signal. Such phenomenon is presented in details in Chapter 5. Excluding the input coupling loss of 1.53 dB, the noise figure near the quantum limit (3.17 dB) is achieved in the system with TBF, indicating a nearly complete suppression of the backward ASE.

Fig. 4.18 illustrates the output signal power as a function of input signal power. The system without optical feedback is able to achieve a higher output power in the unsaturated regime. In this regime, the amplification is linear for all the systems. However, the systems with the optical feedback are able to sustain the linear amplification characteristics up to the input signal power of ~-6 dBm after which the slope changes abruptly. At this input saturation power, the gain of the oscillating

lasers starts to be quenched by the strong injected signal. Without the optical feedback, the slope changes slowly.

In Fig. 4.19, the PCE for the systems operating from the unsaturated regime up to the moderately saturated regime at the maximum pump power P_p = 134.5 mW is presented. For the system without optical feedback, the PCE starts to increase nearly linearly after P_{in} > 30 dBm. The systems with the optical feedback show an exponentially increase beyond $P_{in} \approx$ -25 dBm. The maximum discrepancy in PCE among the systems occurs at $P_{in} \approx$ -15 dBm. A striking feature is that the case shown in Fig. 4.14 is valid only for the unsaturated regime. Operating under the moderately saturated regime ($P_{in} \geq$ -6 dBm), the PCE for the counter-feedback system starts to exceed that of the system without feedback with an amount of 1.4 %. In this saturation regime, the strong input signal starts to quench the gain of the oscillating laser and dominate the cavity.

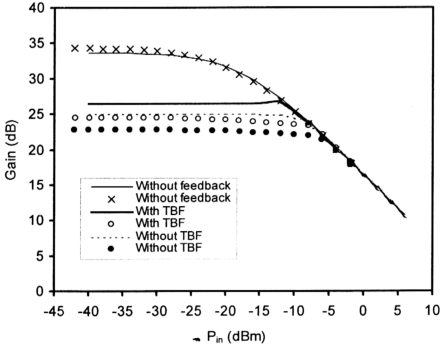

Fig. 4.16 *Signal gain as a function of input signal power for the different feedback schemes with P_p = 134.5 mW and λ_{sig} = 1550 nm. (Point signs: Measured results; lines: Simulation results).*

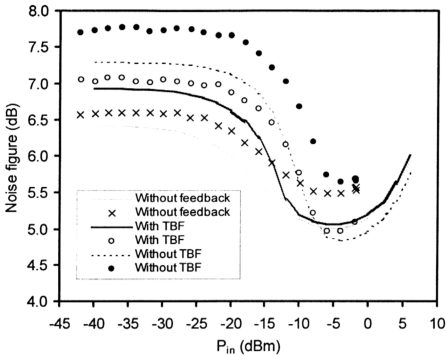

Fig. 4.17 *Noise figure characteristics from the unsaturated to the saturated input signal power with P_p = 134.5 mW and λ_{sig} = 1550 nm. (Point signs: Measured results; lines: Simulation results).*

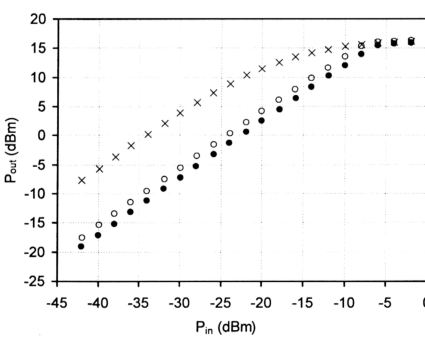

Fig. 4.18 *Output signal power as a function of input signal power with P_p = 134.5 mW and λ_{sig} = 1550 nm. (•: without TBF; o: with TBF; x: without feedback).*

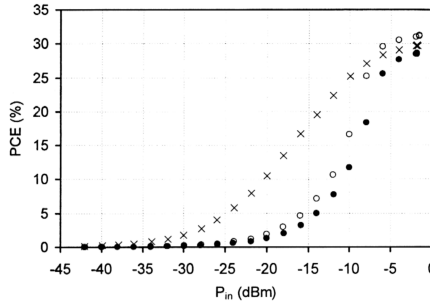

Fig. 4.19 *PCE for the systems operating from the unsaturated regime up to the moderately saturated regime with P_p = 134.5 mW and λ_{sig} = 1550 nm. (•: without TBF; o: with TBF; x: without feedback).*

4.4.3 Effects of Signal Wavelength Variation

The spectral gain characteristic of the EDFAs with different feedback schemes at P_p = 134.5 mW is denoted in Fig. 4.20. The dependence of signal gain on the signal wavelength represents one of the most important EDFA characteristics. The spectral features of the gain spectrum result from the particular absorption and emission cross section line shapes of the EDF and the variation of the gain coefficient along the EDF length, in addition to its loss dependence. Since the unsaturated signal P_{in} = –31.2 dBm is used, the gain spectral follows the profile of the forward ASE spectral. With this small signal, saturation effect is negligible. The system without the optical feedback exhibits a higher signal gain over the entire bandwidth as a result of higher population. Moreover, there is a maximum gain peak of 39.1 dB at the signal wavelength of 1532 nm. This is the wavelength where the emission cross section is the largest. This gain peak can be eliminated by employing gain-flattening filter such

as fiber loop mirror [16], fiber acoustooptic tunable filters [17], or fiber bragg grating [18] so that a wider flat gain spectrum can be utilized for multi-channel amplification in the WDM system. Without the gain-flattening filter, the flat spectral region of 20 nm width can only be obtained at the wavelength range of 1540 nm to 1560 nm. The photon distribution is changed when a feedback loop is introduced. Besides the gain peak at the wavelength of 1532 nm, another high gain regime appears at the wavelength ranging from 1556 nm to 1558 nm as shown in Fig. 4.20.

In Fig. 4.21, noise figure versus signal wavelength is depicted for different schemes at P_p = 134.5 mW and P_{in} = –31.2 dBm. The lowest noise figure is achieved by the system without optical feedback since the inversion level of this scheme is the highest among the systems. The feedback scheme without TBF exhibits the highest noise figure over the entire wavelength range due to the lower clamped-inversion. The high noise figure in the short signal wavelength is due to the low population for the corresponding sub-levels.

Fig. 4.22 shows the PCEs as a function of signal wavelength at the maximum pump power P_p = 134.5 mW. The PCEs for all the systems are relatively low since the unsaturated signal P_{in} = –31.2 dBm is applied. Right-hand-side axis is introduced to clearly indicate the PCE values. Similar to the gain spectrum, the PCEs for all the systems also follow the ASE spectral profile. The system without optical feedback exhibits the highest PCE over the entire amplification bandwidth with the maximum PCE of 4.6 % achieved at the signal wavelength of 1532 nm. As shown in Fig. 4.14, the PCEs for the system with optical feedback decreases with the pump power after the onset of laser oscillation. At the maximum pump power of 134.5 mW, the PCEs are < 0.2 dB for the entire amplification bandwidth.

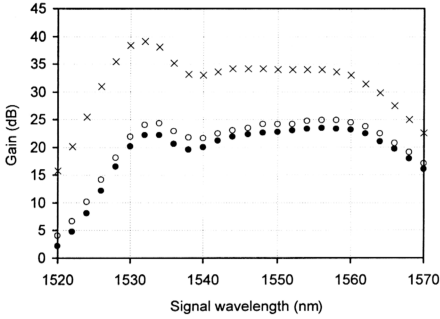

Fig. 4.20 *Dependence of gain on the signal wavelength. P_p = 134.5 mW and P_{in} = -31.2 dBm. (•: without TBF; o: with TBF; x: without feedback).*

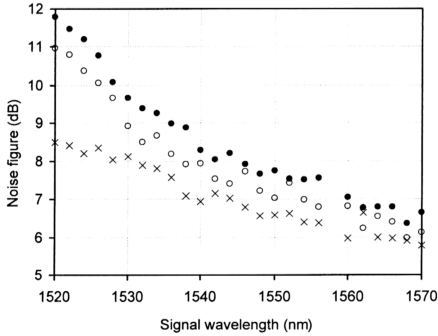

Fig. 4.21 *Noise figure versus signal wavelength for different schemes at P_p = 134.5 mW and P_{in} = -31.2 dBm. (•: without TBF; o: with TBF; x: without feedback).*

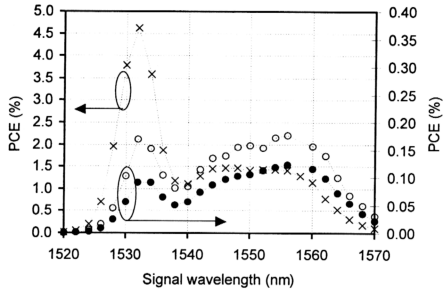

Fig. 4.22 *PCE as a function of signal wavelength at P_p = 134.5 mW and P_{in} = -31.2 dBm. (•: without TBF; o: with TBF; x: without feedback).*

4.5 VARIATION OF LASING WAVELENGTH

4.5.1 Effects of Lasing Wavelength Variation

In this section, the EDFA performance is presented as a function of lasing wavelength λ_{laser} controlled by the tunable bandpass filter in the cavity. The lasing wavelength was determined from the 1 % port of coupler C_3 using the OSA. A probe signal was injected at a fixed wavelength λ_{sig} = 1550 nm and a fixed input signal power P_{in} = –31.2 dBm. Fig. 4.23 shows the gain performance for different pump powers. Since P_p = 89 mW and 134.5 mW are the pump above the lasing threshold, the input signal experiences almost the same gain for both powers over the entire laser tuning range. For P_p = 43.4 mW, the signal gain deviates from the other at the wavelengths shorter than 1530 nm, where the system operates below the lasing threshold. Tuning the lasing wavelengths over the entire amplification bandwidth will actually modify the spectral distribution of the photons in the cavity. This can be seen from the variation of the power level of the output spectrum as shown in Fig. 4.24 at

P_p = 134.5 mW. At λ_{sig} < 1530 nm, the population at the corresponding sub-levels is relatively low. Tuning the lasing wavelength to this regime would not affect too much the population at the wavelength region around 1550 nm. Therefore, the signal gain is high. Fig. 4.24(a) shows the spectrum when the lasing wavelength tuned to λ_{laser} = 1525 nm. The laser power is 8.6 dBm and the ASE level at the wavelength of 1550 nm is 17 dBm. The laser strength is increased to the level of 14.3 dBm when it is tuned to the wavelength region λ_{laser} = 1533 nm where the coefficients of the absorption and emission cross sections are the highest. The population at the 1550 nm region is now affected by such a strong laser. Fig. 4.24(b) indicates that the ASE level reduces to the level of –26 dBm at the wavelength of 1550 nm. The signal gains thus decrease to be ~26.3 dB. When the laser is tuned to λ_{laser} = 1539 nm, a region where a dip appears in the ASE spectrum, the signal gains increase to ~ 28 dB for all the pump powers. At this lasing wavelength, the ASE level is restored to a higher level of –24 dBm. Beyond the lasing wavelength of 1539 nm, the population at the wavelength of 1550 nm becomes dependent on the wavelength detuning of the laser from the input signal. The closer the lasing wavelength to the input signal, the lower the population at the sublevels corresponding to the 1550 nm transition due to the strong stimulated emission by the adjacent oscillating laser mode. In consequence, the signal gain is quenched. However, this is not observed for the lasing wavelength beyond 1550 nm. The signal gains decrease continuously until the lasing wavelength of 1558 nm where there is another gain peak in the ASE spectrum besides the wavelength of 1533 nm. At this wavelength the laser peak power as high as 14.9 dBm is achieved and the signal gains are identical for all the pump powers, that is, 24.1 dB. The signal gains start to increase with a larger detuning.

The noise figure as a function of lasing wavelength for different pump powers are denoted in Fig. 4.25. The noise figure increases with the pump power, consistent with the results shown in Fig. 4.5. The variation of the noise figures versus the lasing wavelength are corresponding to the population variation induced by the oscillating laser with different strength and different detuning parameters. A higher noise figure reveals a lower inversion level at the probe signal wavelength and vice versa. The high noise figure regimes at the wavelength of 1533 nm and at the wavelength range from 1550 nm to 1560 nm are due to strong saturation effect induced by the strong oscillating laser at these two regions. Noise figure as high as 7.4 dB is obtained at the wavelength range of 1550 nm to 1560 nm for the maximum pump P_p = 134.5 mW.

The excess pump power is an appropriate indicator to estimate the pump power that is being absorbed and thus to evaluate the variation of the inversion level. Fig. 4.26 illustrates the excess pump power as a function of lasing wavelength monitored from 980 nm port of WDM II using a power meter as shown in the setup in Fig. 4.1. For the low pump power of 43.4 mW, the excess power variation is relatively small. For the maximum pump power of 134.5 mW, the shape of the plot follows that of the signal gain as shown in Fig. 4.23. At the lasing wavelength λ_{laser} = 1533 nm and the wavelength region from 1550 nm to 1560 nm, the saturation induced by the strong oscillating laser causes a lower inversion level at the metastable level, or in other words, a higher ground state population. This results in a higher pump absorption rate. Therefore, the excess power is minimal under such a condition. The higher excess powers at the lasing wavelengths of 1525, 1539 nm and 1564 nm thus reveal a low ground state population (high inversion level) where the signal gains are high.

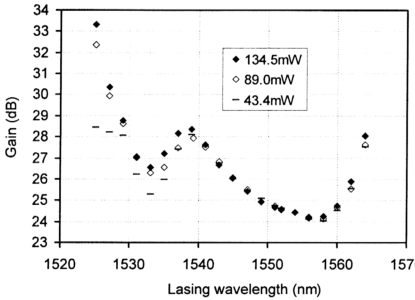

Fig. 4.23 *Gain performance for different pump powers as a function of lasing wavelength. λ_{sig} = 1550 nm and P_{in} = -31.2 dm.*

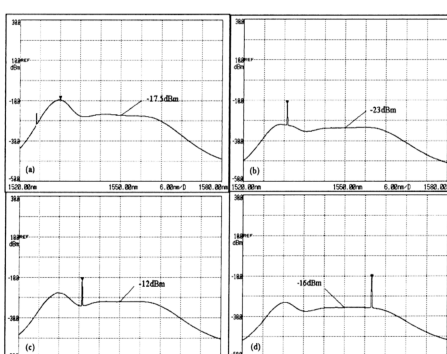

Fig. 4.24 *Output spectrum at P_p = 134.5mW and P_{in} = -31.2 dm. (a) λ_{laser} = 1525 nm, (b) λ_{laser} = 1533 nm, (c) λ_{laser} = 1539 nm, (d) λ_{laser} = 1558 nm.*

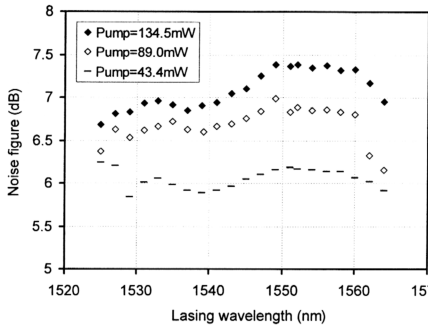

Fig. 4.25 *Noise figure as a function of lasing wavelength for different pump powers. λ_{sig} = 1550 nm and P_{in} = -31.2 dBm.*

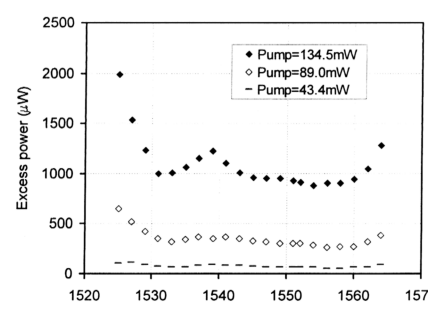

Fig. 4.26 *Excess pump power as a function of lasing wavelength. λ_{sig} = 1550 nm and P_{in} = -31.2 dBm.*

4.5.2 Performance Comparison for Different Lasing Wavelengths

In this section, the amplifier performance among different lasing wavelengths λ_{laser} = 1525 nm, 1533 nm, 1539 nm, 1558 nm and 1564 nm is compared. Fig. 4.27 depicts the signal gain as a function of pump power. The input signal power and signal wavelength is P_{in} = –31.2 dBm and λ_{sig} = 1550 nm, respectively. The signal gains are independent or less dependent on the pump power for the high pump. For λ_{laser} = 1533 nm and 1558 nm, the signal gains are among the lowest (24 dB and 26 dB, respectively), consistent with that illustrated in Fig. 4.23. In addition, the gain-clamping effect starts from a lower pump power $P_p \approx 25$ mW as compared to the cases for other λ_{laser}. For λ_{laser} = 1525 nm, a higher pump power (82.4 mW) is required to achieve the laser oscillation. Therefore, there is still a small gain slope at the high pump powers. The experimental data does not exhibit a sharp threshold or pump power independent signal gain above the lasing threshold for most of the λ_{laser}. Such a behavior can be attributed to spectral hole burning (SHB) [4] induced by the oscillating laser at the laser wavelength that causes an incomplete clamping of the population at the sublevels.

Fig. 4.28 shows the PCE as a function of pump power at different lasing wavelengths interpolated from the data shown in Fig. 4.27. It has been shown in Fig. 4.14 that the PCE of the probe signal can be used to determine the lasing threshold of the oscillator. In Fig. 4.28, the lasing threshold for different lasing wavelengths λ_{laser} = 1525 nm, 1533 nm, 1539 nm, 1558 nm and 1564 nm are determined to be P_{th} = 82.4 mW, 27.0 mW, 36.8 mW, 23.8 mW, 36.8 mW, respectively. Due to the high gain spectral at the wavelengths of 1533 nm and 1558 nm, the laser at these wavelengths is

able to achieve the lasing threshold at a lower pump power. For λ_{laser} = 1525 nm, the laser oscillation still occurs but the pump power as high as 82.4 mW is required.

In Fig. 4.29, noise figures as a function of pump powers is illustrated. The noise figures increase with the pump power for all of the lasing wavelengths. The mechanism for such a phenomenon has been described in previous section. With a low population at the signal wavelength of 1550 nm corresponding to the lasing wavelength of 1533 nm and 1558 nm, the noise figures are among the highest. The lowest noise figure is exhibited when λ_{laser} = 1525 nm.

For a gain-clamped EDFA, it is obviously desirable to have a high P_{in}^{sat} so that amplifier gain control can be maintained over a wide range of input power. Fig. 4.30 shows the dependence of the signal gain on the input signal power P_{in} for the maximum pump power P_p = 134.5 mW and the signal wavelength λ_{sig} = 1550 nm. For the λ_{laser} = 1525 nm, the small-signal gain as high as 33.5 dB is achieved. In this case, the saturation input power P_{in}^{sat} is -17 dBm. The P_{in}^{sat} can be increased by tuning the lasing wavelength to λ_{laser} = 1533 nm or 1558 nm. At these wavelengths, the strong oscillating laser induces a strong gain-clamping effect to the system. Therefore, the P_{in}^{sat} is increased to –7.2 dBm and -5 dBm for λ_{laser} = 1533 nm and 1558 nm, respectively. However, the signal gains are among the lowest: 26.4 dB for λ_{laser} = 1533 nm and 24.4 dB for λ_{laser} = 1558 nm. For effective gain control, it is thus desirable to have a low average inversion.

The noise figure against input signal power is shown in Fig. 4.31. The input signal was varied from –42 dBm to –2 dBm. At this high pump power in such a co-pumping scheme, the noise figure is high in the unsaturated regime due to the high

backward ASE that depopulate the metastable level at the EDF input end. The dips at $P_{in} \approx$ -5 dBm are attributed to the backward ASE suppression by this input power. The population at the EDF input end thus restores back to a higher level. Fig. 4.31 shows that with the lasing wavelength of 1558 nm, a dip with the maximum depth of 2.1 dB is obtained. In this regime, the noise figure at this lasing wavelength is among the lowest although it is not the lowest in the unsaturated regime.

Fig. 4.32 shows the gain spectral with the laser fixed at different wavelengths at P_p = 134.5 mW and P_{in} = -31.2 dBm. Obviously, the population distribution has been modified by different λ_{laser}. By lasing at different wavelengths, various gain distribution can be obtained. The choice of the λ_{laser} not only affects the gain distribution, but also the achievable gain value. At λ_{laser} = 1525 nm, where the laser power is weak, the population is the highest over the entire amplification bandwidth with the 1533 nm region exhibits the highest signal gain. Signal gain as high as 33.4 dB is achieved in the flat gain region ranging from 1544 nm to 1558 nm. By tuning the lasing wavelength to λ_{laser} = 1558 nm, the lowest threshold inversion for this λ_{laser} causes the lowest signal gain among different λ_{laser}. In this case, the signal experiences the same gain (25 dB) when λ_{laser} = 1533 nm and 1558 nm. Although it is desirable to have a low inversion level for effective gain control, the relatively longer λ_{laser} = 1558 nm causes deep saturation and a less uniform gain spectrum. To improve the gain flatness, a relatively short λ_{laser} must be selected to maintain a relatively high average population inversion. However, this is compensated at a cost of smaller dynamic range as shown in Fig. 4.30.

The noise figure versus signal wavelength is denoted in Fig. 4.33. With the lowest population inversion exhibited by fixing the lasing wavelength at λ_{laser} =

1558 nm, the noise figure achieved is among the highest especially at the short signal wavelengths. High inversion level is preserved when λ_{laser} = 1525 nm is selected. It is evident that the noise figure at this λ_{laser} is among the lowest as a consequence of the smaller saturation effect.

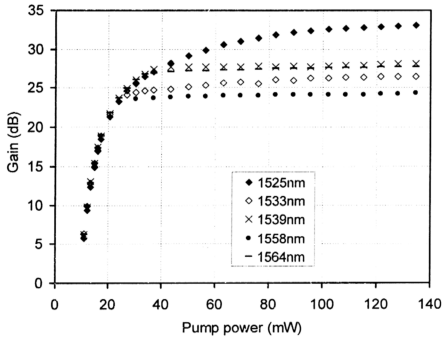

Fig. 4.27 *Signal gain as a function of pump power with different lasing wavelengths. λ_{sig} = 1550 nm and P_{in} = -31.2 dBm.*

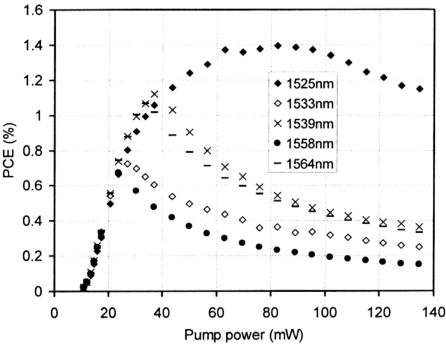

Fig. 4.28 *PCE as a function of pump power for different lasing wavelengths. λ_{sig} = 1550 nm and P_{in} = -31.2 dBm.*

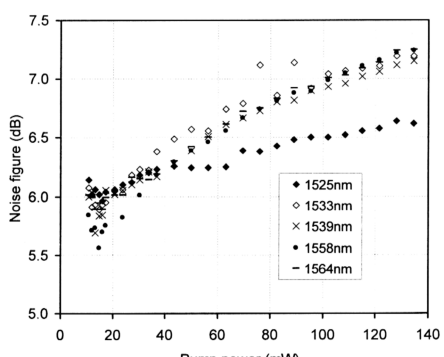

Fig. 4.29 *Noise figures of the input signal as a function of pump powers. λ_{sig} = 1550 nm and P_{in} = -31.2 dBm.*

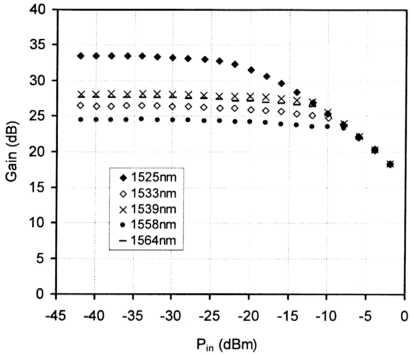

Fig. 4.30 *Dependence of the signal gain on the input signal power. λ_{sig} = 1550 nm and P_{in} = -31.2 dBm.*

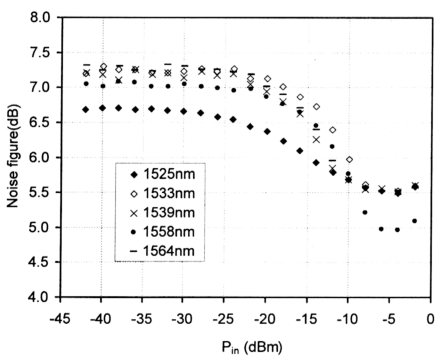

Fig. 4.31 *The noise figure against input signal power. λ_{sig} = 1550 nm and P_p = 134.5 mW.*

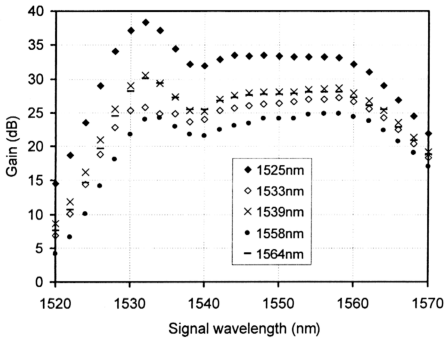

Fig. 4.32 *Gain spectral with the laser fixed at different wavelengths. P_p = 134.5 mW and P_{in} = -31.2 dBm.*

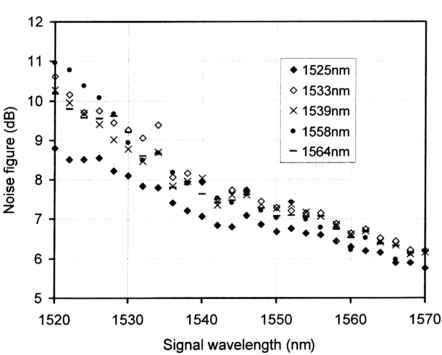

Fig. 4.33 *Noise figure versus signal wavelength with the laser fixed at different wavelengths. P_p = 134.5 mW and P_{in} = -31.2 dBm.*

4.6 CONCLUSIONS

Erbium-doped fiber amplifier with optical counter-feedback has been presented. Although the oscillating laser was supposed to be eliminated at the amplifier output in such a feedback scheme, back reflection caused the oscillating laser existing at the amplifier output. Comparison with the system without feedback showed that signal gain and noise figure were deteriorated. The lower signal gain was due to the clamping of the inversion at a lower level after the onset of laser oscillation whereas degradation in the noise figure could be attributed to the laser-induced saturation at the EDF input end. However, the existence of the oscillating laser induced the gain clamping effect, resulting in an increase in the dynamic range where the linear amplification could be sustained up to a fairly high input signal level before getting saturated. With the tunable bandpass filter in the cavity, the desired amplifier performance, including the signal gain, noise figure, gain flatness and dynamic range could be achieved by choosing an appropriate lasing wavelength.

REFERENCES

[1] Y. Sun, A. K. Srivastava, J. L. Zyskind, J. W. Sulholf, C. Wolf and R. W. Tkach, "Fast power transients in WDM optical networks with cascaded EDFA's," Electron. Lett., 33, pp. 313, 2000.

[2] A. K. Srivastava, J. L. Zyskind, Y. Sun, J. Ellson, G. Newsome, R. W. Tkach, A. R. Chraplyvy, J. W. Sulholf, T. A. Strasser, C. Wolf and ad J. R. Pedrazzani, "Fast-link control protection of surviving channels in multiwavelength optical networks," IEEE Photon. Technol. Lett., 9, pp. 1667, 1997.

[3] M. Karásek and J. A. Vallés, "Analysis of Channel Addition/Removal Response in All-Optical Gain-Controlled Cascade of Erbium-Doped Fiber Amplifiers," J. Light. Technol., 16, pp. 1795, 1998.

[4] M. F. Krol, Y. Liu, J. J. Watkins and M. J. Dalley, "Gain Variation in Optically Gain Clamped Erbium Doped Fiber Amplifiers." ECOC'98, pp. 43, 1998; M. F. Krol, Y. Q. Liu, J. J. Watkins and D. W. Lambert, "Dual cavity optical automatic gain control for EDFA," OFC/IOOC '99. Technical Digest , 2, pp. 214 , 1999.

[5] A. Yu and M. J. O'Mahony, "Properties of gain controlled erbium doped fiber amplifiers by lasing" Electron. Lett., 31, pp. 1348, 1995.

[6] M. Cai, X. Liu, J. Cui, P. Tang, and J. Peng, "Study on noise characteristic of gain-clamped erbium-doped fiber-ring lasing amplifier," IEEE Photonics. Technol. Lett., 9, pp. 1093, 1997.

[7] T. C. Teyo, M. A. Mahdi, P. Poopalan, and H. Ahmad, "Properties of laser and amplified signal in a gain-clamped Er^{3+}-doped fiber amplifier system,"

Microwave Opt. Technol. Lett., 26, pp. 418, 2000.

[8] E. Delevaque, T. Georges, J. F. Bayon, M. Monerie, P. Niay, and P. Bernage, "Gain-control in erbium doped fiber amplifiers by lasing at 1480 nm with photoinduced bragg grating written on fiber end," Electron. Lett., 29, pp. 1112, 1993.

[9] J. Massicott, C. Lebre, R. Wyatt, R. Kashyap, D. Williams, and A. Yu, "Low noise, all-optical gain controlled Er^{3+} doped fiber amplifier using asymmetric control laser cavity design," Electron. Lett., 32, pp. 816, 1996; S. Y. Ko, M. W. Kim, D. H. K., S. H. Kim, J. C. Jo and J. H. Park, "Gain control in erbium-doped fiber amplifiers by tuning center wavelength of a fiber Bragg grating constituting resonant cavity," Electron. Lett., Vol. 34, pp. 990, 1998.

[10] Kyo Inoue, "Gain-Clamped Fiber Amplifier with a Loop Mirror Configuration," IEEE Photon. Technol. Lett., 11, pp. 533, 1999.

[11] A. E. Siegman, Lasers, University Science Books, CA, 1986.

[12] R. G. Smart, J. L. Zyskind, J. W. Sulhoff, and D. J. DiGiovanni, "An Investigation of the Noise Figure and Conversion Efficiency of 0.98 μm Pumped Erbium-Doped Fiber Amplifiers Under Saturated Conditions," IEEE Photon. Technol. Lett., 4 pp. 1261, 1992.

[13] E. Desurvire, "Erbium-doped Fiber Amplifiers – Principles and Applications," John Wiley & Sonc, Inc., 1994.

[14] R. I. Laming, J. E. Townsend, D. N. Payne, F. Meli, G. Grasso and E. J. Tarbox, "High Power Erbium-Doped Fiber Amplifiers Operating in the Saturated Regime," 3, pp. 253, 1991.

[15] Tuan Chin TEYO, Mun Kiat LEONG and Harith AHMAD, "Noise Characteristics of

Erbium-Doped Fiber Amplifier with Optical Counter-Feedback," Jpn. J. Appl. Phys. 41, Part 1, No. 5A, pp. 2949, 2002.

[16] Shenping Li, K. S. Chiang, W.A Gambling, "Gain flattening of an erbium-doped fiber amplifier using a high-birefringence fiber loop mirror," IEEE Photon. Technol. Lett. 13, pp.942, 2001.

[17] S. H. Yun, B. W. Lee, H. K. Kim, B. Y. Kim, "Dynamic erbium-doped fiber amplifier based on active gain flattening with fiber acoustooptic tunable filters," IEEE Photon. Lett. 11. pp. 1229, 1999.

[18] R. Kashyap, R. Wyatt, R. J. Campbell, "Wideband gain flattened erbium fibre amplifier using a photosensitive fibre blazed grating," Electron. Lett., 29, pp. 154, 1993.